Supporting Information

Intermolecular Interactions at the Interface Quantified by Surface-sensitive Second-Order Fermi Resonant Signals

Kangzhen Tian,[1, 2] Baixiong Zhang,[1] Shuji Ye,[1,2,*] Yi Luo[1,2]

[1]Hefei National Laboratory for Physical Sciences at the Microscale, and Department of Chemical Physics, University of Science and Technology of China, Hefei, Anhui, P.R.China 230026 & [2]Synergetic Innovation Center of Quantum Information & Quantum Physics, University of Science and Technology of China, Hefei, Anhui 230026, China

1. Lipid molecular structures

DLPA

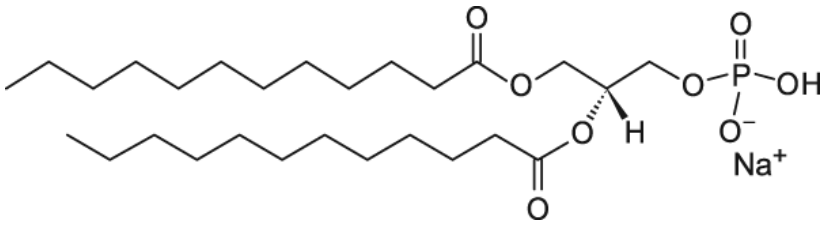

DMPA

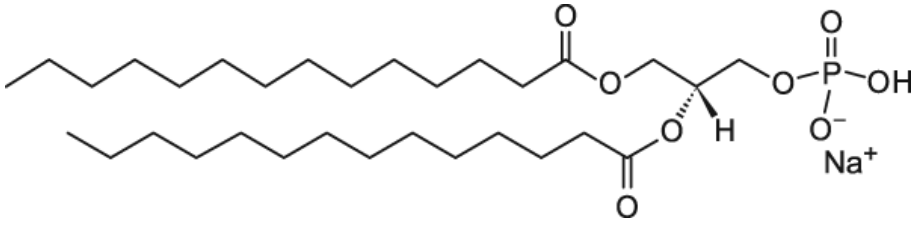

DPPA

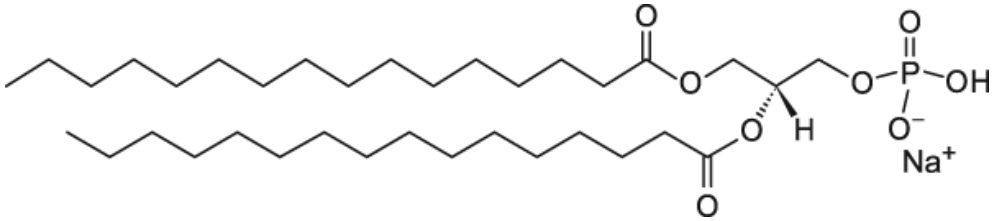

DSPA

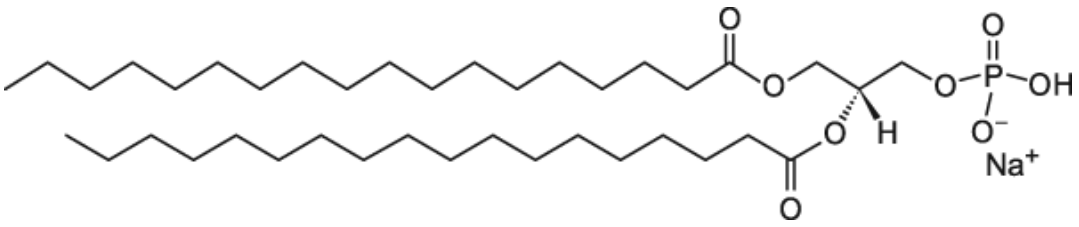

DLPC

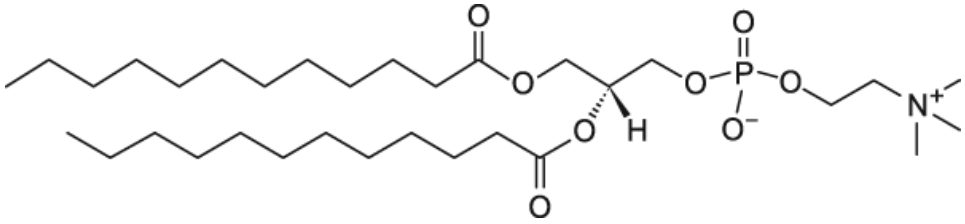

Figure S1 Lipid molecular structure

2. Fitting of SFG-VS Signal

As described in detail elsewhere, [1-6] the intensity of the SFG light is related to the square of the sample's second-order nonlinear susceptibility ($\chi^{(2)}_{eff}$), and the intensity of the two input fields $I(\omega_{IR})$ and $I(\omega_{Vis})$, see eq. (S1), which vanishes when a material has inversion symmetry.

$$I(\omega_{SFG}) \propto \left|\chi^{(2)}_{eff}\right|^2 I_1(\omega_{Vis}) I_2(\omega_{IR}) \quad \text{(S1)}$$

where $\omega_{SFG} = \omega_{IR} + \omega_{Vis}$. As the IR beam frequency is tuned over the vibrational resonance of surface/interface molecules, the effective surface nonlinear susceptibility $\chi^{(2)}_R$ can be enhanced. The frequency dependence of $\chi^{(2)}_{eff}$ is described by eq. (S2).

$$\chi^{(2)}_{eff}(\omega) = \chi^{(2)}_{NR} + \sum_{\upsilon} \frac{A_\upsilon}{\omega - \omega_\upsilon + i\Gamma_\upsilon} \quad \text{(S2)}$$

where A_υ, ω_υ, and Γ_υ are the strength, resonant frequency, and damping coefficient of the vibrational mode (ν), respectively. A_υ could be either positive or negative depending on the phase of the vibrational mode. The plot of SFG signal vs. the IR input frequency shows a polarized vibrational spectrum of the molecules at surface or interface. A_υ, ω_υ, and Γ_υ can

be extracted by fitting the spectrum.

3. The method to accurately determine Fermi resonance by suppressing asymmetric signal of methyl group

SFG susceptibility tensor elements $\chi_{ijk}(i,j,k=x,y,z)$ can be described as a function of the molecular orientation and the SFG molecular hyperpolarizability tensor elements $\beta_{lmn}(l,m,n=a,b,c)$. For a methyl group with C_{3v} symmetry, the SFG susceptibility tensor elements $\chi_{ijk}(i,j,k=x,y,z)$ of C_{3v} symmetry have following relationships.[1-6]

Symmetric stretch mode:

$$\chi^{(2)}_{xxz,ss} = \chi^{(2)}_{yyz,ss} = \frac{1}{2}N_s[(1+r)<\cos\theta> -(1-r)<\cos^3\theta>]\beta_{ccc} \quad \text{(S3)}$$

$$\chi^{(2)}_{zzz,ss} = N_s[r<\cos\theta> +(1-r)<\cos^3\theta>]\beta_{ccc} \quad \text{(S4)}$$

Asymmetric stretch mode:

$$\chi^{(2)}_{xxz,as} = \chi^{(2)}_{yyz,as} = -N_s[<\cos\theta> - <\cos^3\theta>]\beta_{aca} \quad \text{(S5)}$$

$$\chi^{(2)}_{zzz,as} = 2N_s[<\cos\theta> - <\cos^3\theta>]\beta_{aca} \quad \text{(S6)}$$

Here $r = \beta_{aac}/\beta_{ccc}$. On the other hand, the SFG signal intensity can be expressed in terms of an effective nonlinear susceptibility ($\chi^{(2)}_{eff}$). The components of $\chi^{(2)}_{eff}$ for co-propagation geometry are given in eq.(S7) in the lab coordinate system which is defined as the z-axis being along the surface normal and the x-axis being in the incident plane (Figure S2).[1-9]

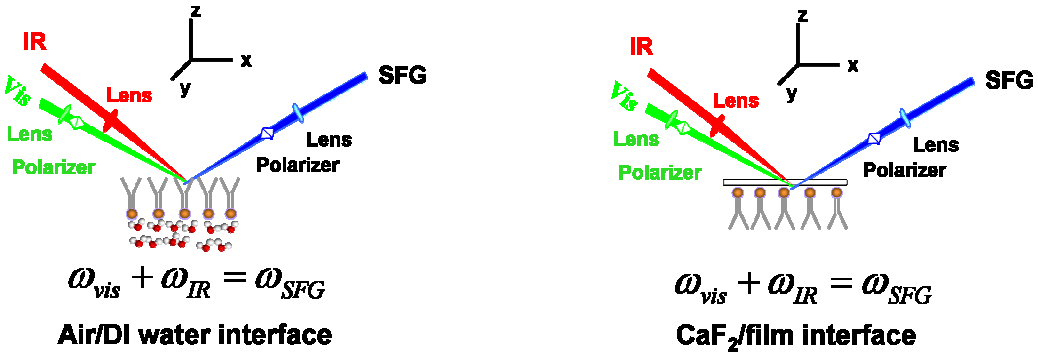

Figure S2. Schematics of the SFG experimental geometry.

$$
\begin{aligned}
\chi_{eff}^{(2)} = & \sin\Omega_{SF}\sin\Omega_{Vis}\cos\Omega_{IR}L_{yy}(\omega_{SF})L_{yy}(\omega_{Vis})L_{zz}(\omega_{IR})\sin\beta_{IR}\chi_{yyz}^{(2)} \\
& + \sin\Omega_{SF}\cos\Omega_{Vis}\sin\Omega_{IR}L_{yy}(\omega_{SF})L_{zz}(\omega_{Vis})L_{yy}(\omega_{IR})\sin\beta_{Vis}\chi_{yzy}^{(2)} \\
& + \cos\Omega_{SF}\sin\Omega_{Vis}\sin\Omega_{IR}L_{zz}(\omega_{SF})L_{yy}(\omega_{Vis})L_{yy}(\omega_{IR})\sin\beta_{SF}\chi_{zyy}^{(2)} \\
& - \cos\Omega_{SF}\cos\Omega_{Vis}\cos\Omega_{IR}L_{xx}(\omega_{SF})L_{xx}(\omega_{Vis})L_{zz}(\omega_{IR})\cos\beta_{SF}\cos\beta_{Vis}\sin\beta_{IR}\chi_{xxz}^{(2)} \\
& - \cos\Omega_{SF}\cos\Omega_{Vis}\cos\Omega_{IR}L_{xx}(\omega_{SF})L_{zz}(\omega_{Vis})L_{xx}(\omega_{IR})\cos\beta_{SF}\sin\beta_{Vis}\cos\beta_{IR}\chi_{xzx}^{(2)} \\
& + \cos\Omega_{SF}\cos\Omega_{Vis}\cos\Omega_{IR}L_{zz}(\omega_{SF})L_{xx}(\omega_{Vis})L_{xx}(\omega_{IR})\sin\beta_{SF}\cos\beta_{Vis}\cos\beta_{IR}\chi_{zxx}^{(2)} \\
& + \cos\Omega_{SF}\cos\Omega_{Vis}\cos\Omega_{IR}L_{zz}(\omega_{SF})L_{zz}(\omega_{Vis})L_{zz}(\omega_{IR})\sin\beta_{SF}\sin\beta_{Vis}\sin\beta_{IR}\chi_{zzz}^{(2)}
\end{aligned}
\tag{S7}
$$

where the parameters Ω_{SF}, Ω_{Vis} and Ω_{IR} are the polarization angles of the SFG signal, visible, and IR laser beam, respectively. β_{SF}, β_{Vis}, and β_{IR} are the angles between the surface normal and the sum frequency beam, the input visible beam, and the input IR beam, respectively. L_{ii} (i = x, y or z) denotes the Fresnel coefficients. The polarization combination is ssp for Ω_{SF} = Ω_{Vis} = 90° and Ω_{IR} = 0°, whereas ppp for Ω_{SF} = Ω_{Vis} = Ω_{IR} = 0°. In our experimental geometry, we have the following relationship.

$$
\begin{aligned}
& L_{xx}(\omega_{SF})L_{zz}(\omega_{Vis})L_{xx}(\omega_{IR})\cos\beta_{SF}\sin\beta_{Vis}\cos\beta_{IR}\chi_{xzx}^{(2)} \\
& \approx L_{zz}(\omega_{SF})L_{xx}(\omega_{Vis})L_{xx}(\omega_{IR})\sin\beta_{SF}\cos\beta_{Vis}\cos\beta_{IR}\chi_{zxx}^{(2)}
\end{aligned}
\tag{S8}
$$

If we rotate the polarization angle of sum frequency output to 45°, and keep the infrared at *p* or 0°, then the generated susceptibility ($\chi_{eff}^{(2)}$) can be expressed as

$$
\begin{aligned}
\chi_{eff}^{(2)}(45^\circ\,\Omega_{Vis}\,p) = & \frac{\sqrt{2}}{2}\sin\Omega_{Vis}L_{yy}(\omega_{SF})L_{yy}(\omega_{Vis})L_{zz}(\omega_{IR})\sin\beta_{IR}\chi_{yyz}^{(2)} \\
& - \frac{\sqrt{2}}{2}\cos\Omega_{Vis}L_{xx}(\omega_{SF})L_{xx}(\omega_{Vis})L_{zz}(\omega_{IR})\cos\beta_{SF}\cos\beta_{Vis}\sin\beta_{IR}\chi_{xxz}^{(2)} \\
& + \frac{\sqrt{2}}{2}\cos\Omega_{Vis}L_{zz}(\omega_{SF})L_{zz}(\omega_{Vis})L_{zz}(\omega_{IR})\sin\beta_{SF}\sin\beta_{Vis}\sin\beta_{IR}\chi_{zzz}^{(2)}
\end{aligned}
\tag{S9}
$$

According to the equations of (S5) and (S6), the asymmetric stretch of the methyl group has a relationship of $\chi_{zzz,as}^{(2)} = -2\chi_{yyz,as}^{(2)}$. It is therefore possible to find one set of the polarization angles of the SFG signal, visible and IR laser beam to satisfy $\chi_{eff,as}^{(2)} = 0$ in Eq.S10 after considering the Fresnel coefficient constants under the experimental geometry and assuming that orientation of CH_3 group follows a δ-distribution.

$$\chi_{eff}^{(2)}(45^{\circ}\Omega_{Vis}p)_{as} / \chi_{yyz,as}^{(2)} = \sin\Omega_{Vis}\left[\frac{\sqrt{2}}{2}L_{yy}(\omega_{SF})L_{yy}(\omega_{Vis})L_{zz}(\omega_{IR})\sin\beta_{IR}\right]$$
$$-\cos\Omega_{Vis}\left[\begin{array}{l}\frac{\sqrt{2}}{2}L_{xx}(\omega_{SF})L_{xx}(\omega_{Vis})L_{zz}(\omega_{IR})\cos\beta_{SF}\cos\beta_{Vis}\sin\beta_{IR}\\+\sqrt{2}\cos\Omega_{Vis}L_{zz}(\omega_{SF})L_{zz}(\omega_{Vis})L_{zz}(\omega_{IR})\sin\beta_{SF}\sin\beta_{Vis}\sin\beta_{IR}\end{array}\right] \quad \text{(S10)}$$

It is worth mentioning that although we assumed the orientation distribution as a δ-distribution, it is in fact very narrow because the molecular distribution in Langmuir monolayer is generally azimuthally isotropic.[10, 11] At this case, the CH_3 asymmetric signals will be suppressed theoretically. The solution for the polarization angles of the SFG signal, visible and IR laser beams to satisfy $I(45^{\circ}\Omega_{Vis}p), as = 0$ is Ω_{Vis} = 74°~76°. Depending on the reflective index of the surface, the value of Ω_{Vis} in experiments may have several degree difference compared to the theoretical prediction. In addition, Prof. H. F. Wang group found that the design of the original experimental setup of the SFG spectrometer by EKSPLA Company could not control accurately the polarizations of the incident beams other than s or p polarization.[12] The intended –45° polarization of the 532 nm incident beam was controlled by a half wave plate (HWP) far from the sample, after six 45°coated reflecting mirrors and two total internal interfaces of a prism before being focused on to the liquid interface. The polarization at the sample is thus affected. Wang Group improved the polarization control by changing the position of the HWP close to the focal lens, and make frequent calibration of the polarization angles.

4. Table S1- Table S4

Table S1. The molecular interaction of the lipid monolayer deposited at CaF_2 windows

Lipids	n_C	MMA(A_L) (nm^2)	r_{ij}^{chain} (nm)	E_{vdw} (kJ/mol)	E_{el} (kJ/mol)
DLPA	12	0.4858	0.5561	-19.93	constant
DMPA	14	0.4580	0.5400	-27.39	constant
DPPA	16	0.3930	0.5002	-47.77	constant
DSPA	18	0.3654	0.4823	-65.62	constant

Table S2. The molecular interaction of the DLPC monolayer at air/water interface at different surface pressure

surface pressure (mN/m)	MMA (A_L) (nm^2)	r_{ij}^{chain} (nm)	$1/r_{ij}^{chain}$ (1/nm)	E_{vdw} (kJ/mol)	E_{el} (kJ/mol)
0.05	1.1645	0.861	1.1614	-1.666	negligible
0.5	1.0379	0.8129	1.2302	-2.322	negligible
1	1.0097	0.8018	1.2473	-2.513	negligible
5	0.8867	0.7513	1.3310	-3.647	negligible
10	0.7986	0.7130	1.4025	-4.917	negligible
20	0.6927	0.6641	1.5059	-7.365	negligible
30	0.6252	0.6309	1.5851	-9.838	negligible
40	0.5704	0.6026	1.6595	-12.731	negligible

Table S3. The molecular interaction of the DLPC monolayer at air/soluton interface at different salt solution (20 mM) at 10mN/m.

salt	MMA (A_L)(nm^2)	r_{ij}^{chain} (nm)	Δπ(mN/m)	E_{vdw} (kJ/mol)	E_{el} (kJ/mol)	$E_{vdW} + E_{el}$ (kJ/mol)
H_2O	0.7986	0.7130	0	-4.917	0	-4.917
K_2SO_4	0.8095	0.7179	0.777	-4.731	0.379	-4.352
KCl	0.8330	0.7282	2.206	-4.360	1.107	-3.253
KBr	0.8744	0.7461	4.436	-3.796	2.336	-1.460
KNO_3	0.9143	0.7629	6.137	-3.341	3.379	0.038
KI	0.9699	0.7858	8.02	-2.821	4.684	1.863
$KClO_4$	1.0289	0.8093	9.353	-2.381	5.795	3.414
KSCN	1.0774	0.8282	9.863	-2.085	6.399	4.314

Table S4. The molecular interaction of the DLPC monolayer at air/soluton interface at different salt solution(100 mM) at 10mN/m.

salt	MMA (nm^2)	r_{ij}^{chain} (nm)	Δπ(mN/m)	E_{vdw} (kJ/mol)	E_{el} (kJ/mol)	$E_{vdW} + E_{el}$ (kJ/mol)
H_2O	0.7986	0.7130	0	-4.917	0	-4.917
K_2SO_4	0.87869	0.7479	4.646	-3.743	2.458	-1.285
KCl	0.91677	0.7640	6.235	-3.315	3.442	0.127
KBr	0.95658	0.7804	7.617	-2.935	4.388	1.453
KNO_3	0.981	0.7903	8.305	-2.730	4.906	2.176
KI	1.049	0.8172	9.657	-2.252	6.100	3.848
$KClO_4$	1.134	0.8497	9.94	-1.799	6.788	4.989
KSCN	1.182	0.8675	9.955	-1.596	7.086	5.49

5. Figure S3-Figure S9

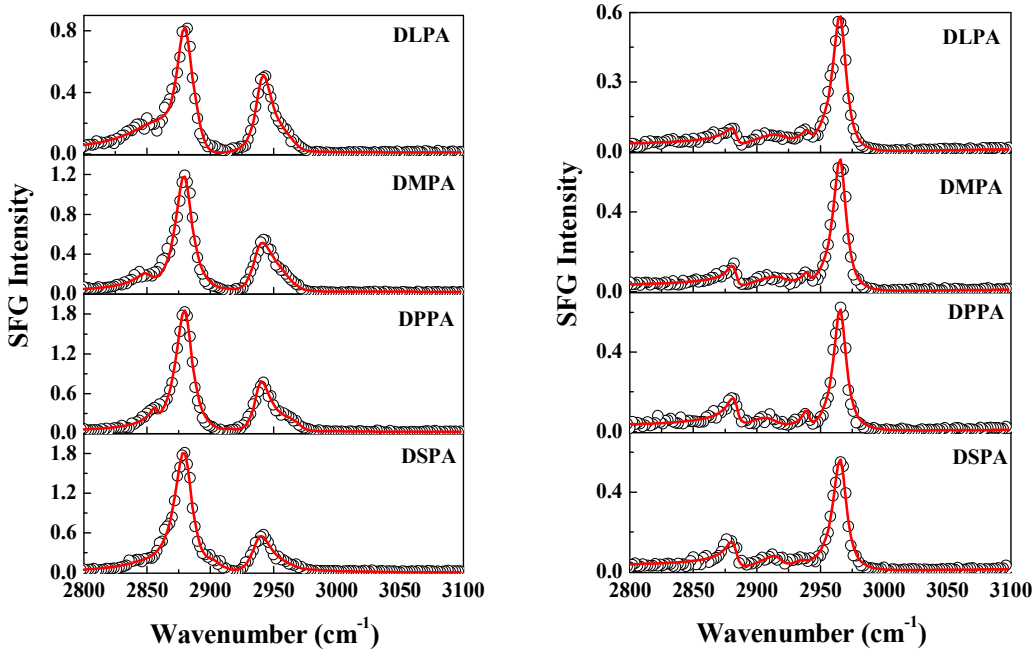

Figure S3. The ssp and ppp SFG spectra of lipid Langmuir monolayer films deposited at CaF_2 windows at the surface pressure of 30 mN/m.

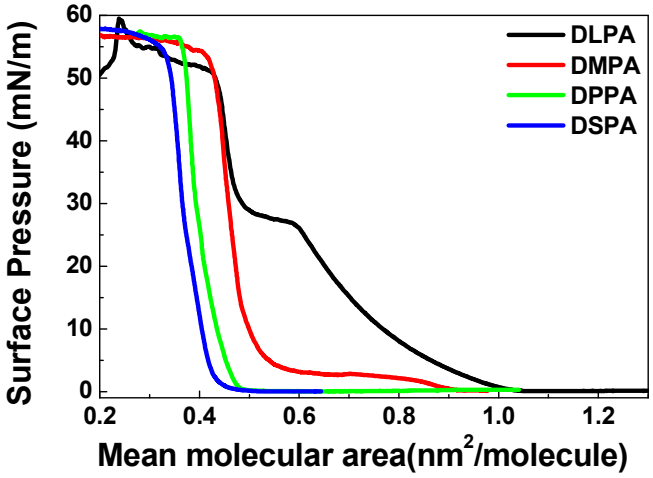

Figure S4. The surface pressure-area (π-A) isotherms of PA lipid monolayer at air/DI water interface.

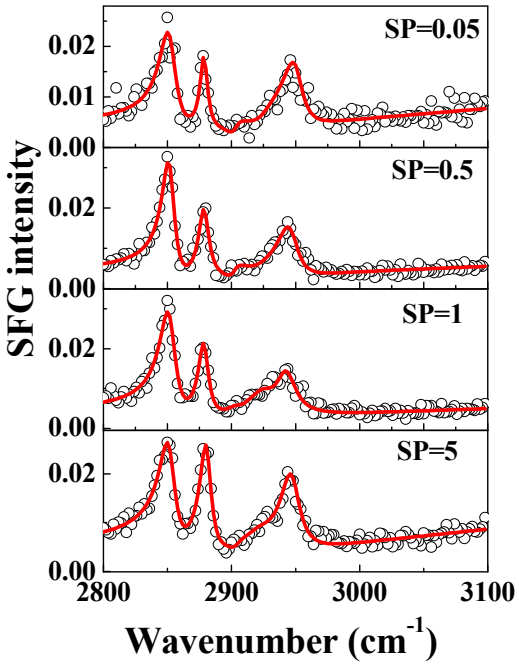

Figure S5. The 45°76°p SFG spectra of DLPC Langmuir monolayer at air /DI water interface at different surface pressures.

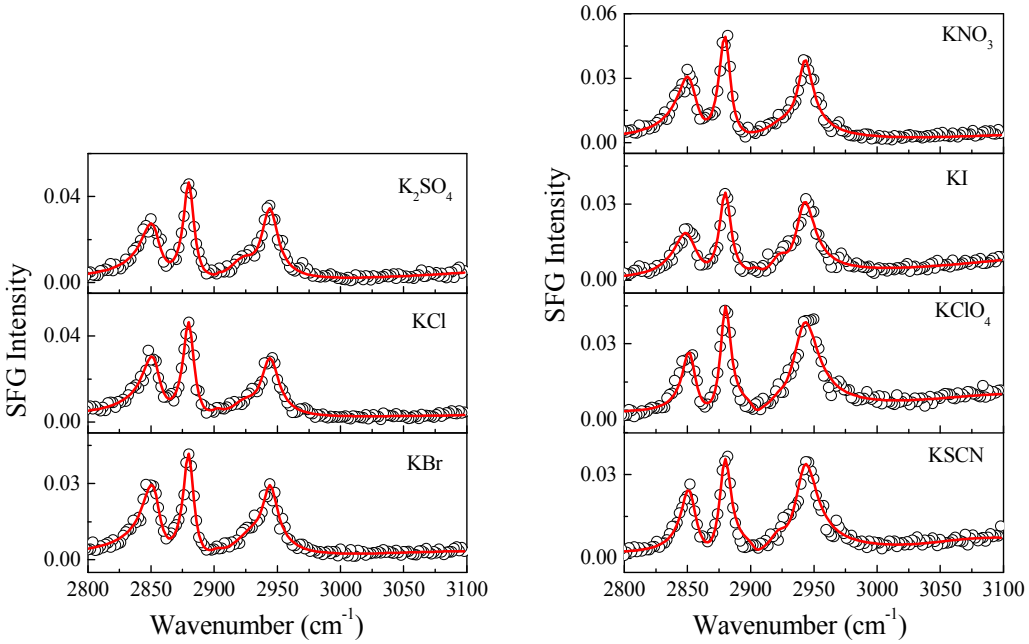

Figure S6. The 45°76°p SFG spectra of DLPC Langmuir monolayer at air /salt solution (20 mM) interface at the surface pressures of 10 mN/m.

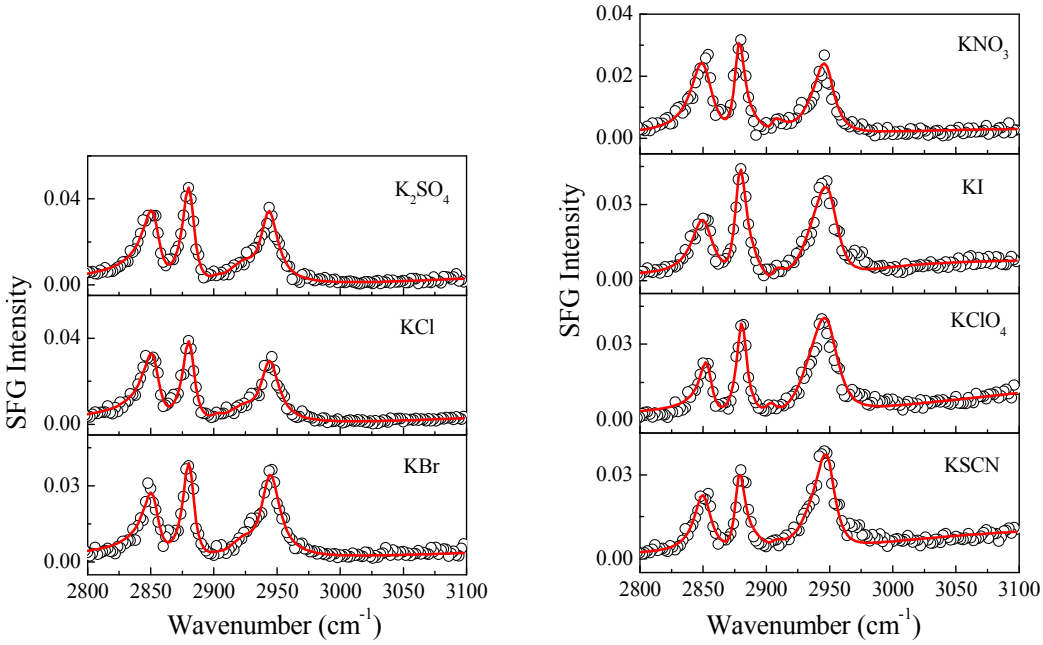

Figure S7. The 45°76°p SFG spectra of DLPC Langmuir monolayer at air /salt solution (100 mM) interface at the surface pressures of 10 mN/m.

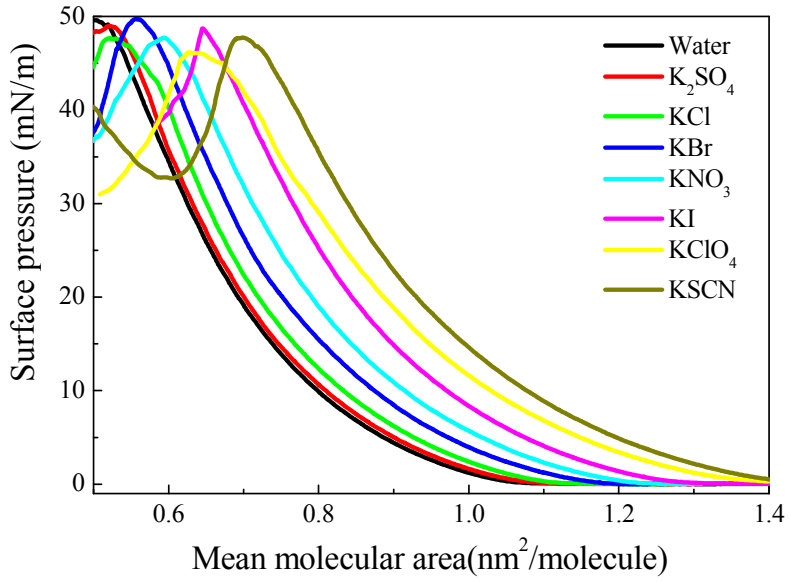

Figure S8. The surface pressure-area (π-A) isotherms of DLPC lipid monolayer at air/solution interface with ionic strength of 20 mM.

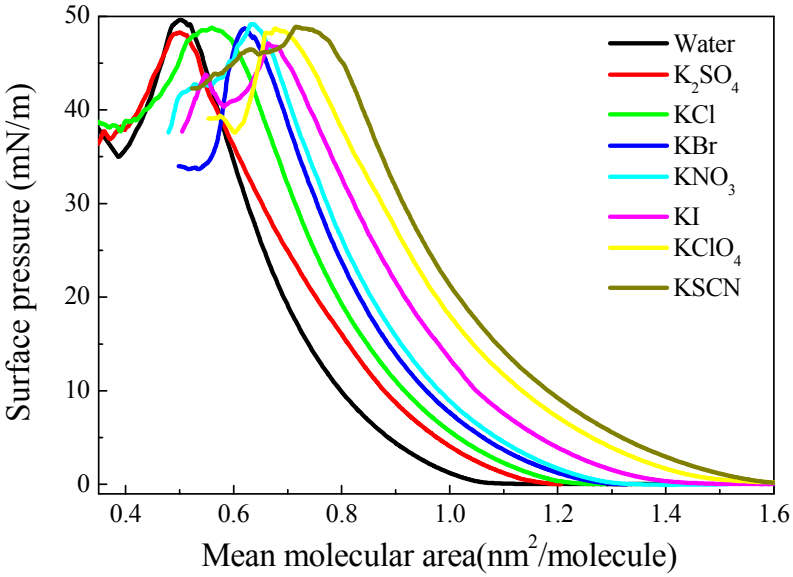

Figure S9. The surface pressure-area (π-A) isotherms of DLPC lipid monolayer at air/solution interface with ionic strength of 100 mM.

6. The orientation of the terminal methyl group in different salt solution

The molecular orientation of the terminal methyl group can be determined using the

measured ppp and ssp spectral intensity ratios ($\chi^{(2)}_{ppp}(CH_3,as)/\chi^{(2)}_{ssp}(CH_3,ss)$), which is the common procedures that most people did in the literatures.[13,14] Because the methyl groups obey the relationship of $\chi^{(2)}_{xxz}=\chi^{(2)}_{yyz}$ and $\chi^{(2)}_{zzz,as}=-2\chi^{(2)}_{yyz,as}$, according to Eqs.(S3)-(S6), we can reach the following equations of Eq.(S11) and Eq.(S12) after considering the Fresnel coefficient constants. Hence, the orientation angles of the terminal methyl group can be determined according to a relation between the $\chi^{(2)}_{ppp}(CH_3,as)/\chi^{(2)}_{ssp}(CH_3,ss)$ and θ_{CH_3} (Eq.(S12)). The result is given in Table S5.

$$\frac{\chi^{(2)}_{ppp}(CH_3,as)}{\chi^{(2)}_{ssp}(CH_3,ss)}=\frac{-0.1534\chi^{(2)}_{xxz,as}+0.2083\chi^{(2)}_{zzz,as}}{0.2405\chi^{(2)}_{yyz,ss}}=\frac{-0.57\chi^{(2)}_{yyz,as}}{0.2405\chi^{(2)}_{yyz,ss}} \quad \text{(S11)}$$

$$\frac{\chi^{(2)}_{ppp}(CH_3,as)}{\chi^{(2)}_{ssp}(CH_3,ss)}=\frac{-0.57\chi^{(2)}_{yyz,as}}{0.2405\chi^{(2)}_{yyz,ss}}=\frac{45.79(<\cos\theta>-<\cos^3\theta>)}{3.3<\cos\theta>+1.3<\cos^3\theta>} \quad \text{(S12)}$$

It is evident that the orientations of the terminal methyl group at the air/DI water interface and the air/salt solution interface change very small (θ = 21±1°). Therefore, the influence of the orientation of the terminal methyl group on the value of the ratio $R_{2v2/v1}$ will be very small.

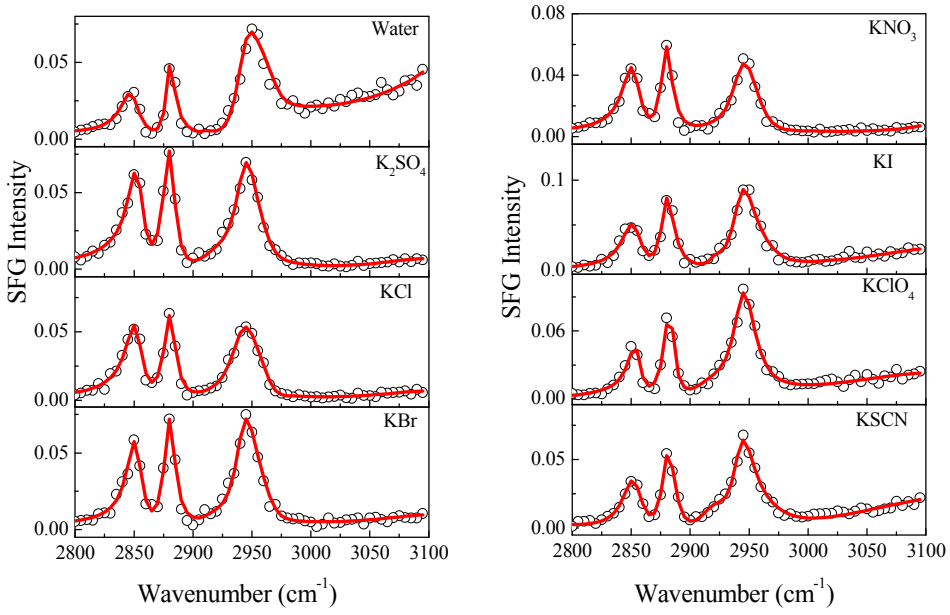

Figure S10. The ssp SFG spectra of DLPC Langmuir monolayer at air /salt solution (100 mM) interface at the surface pressures of 10 mN/m.

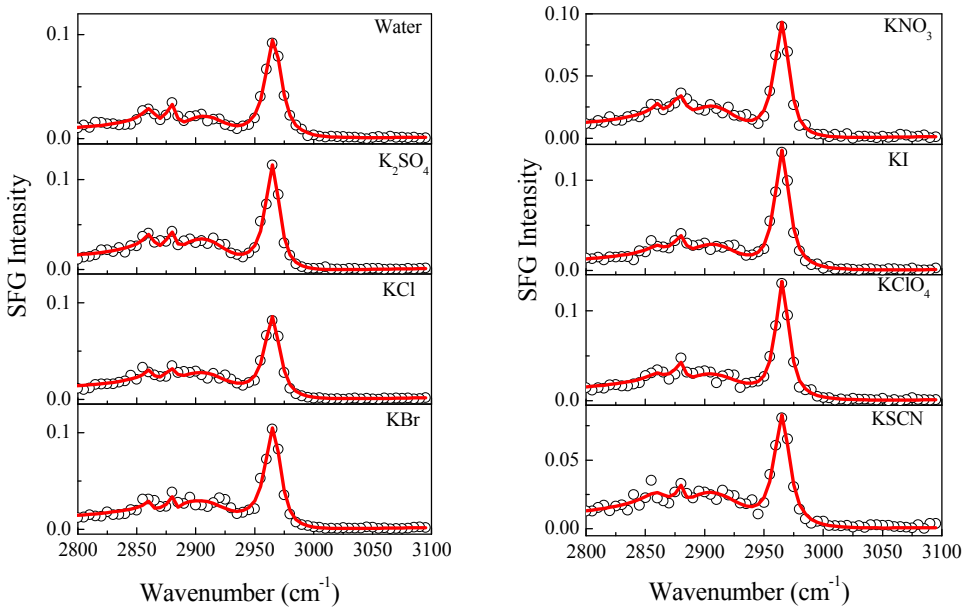

Figure S11. The ppp SFG spectra of DLPC Langmuir monolayer at air /salt solution (100 mM) interface at the surface pressures of 10 mN/m.

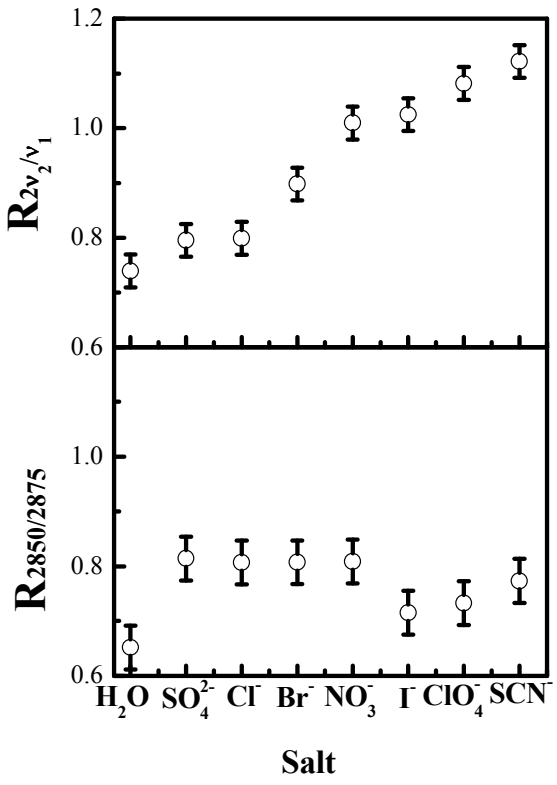

Figure S12. The intensity ratios ($R2\nu_2/\nu_1$) and $R_{2850/2875}$ of DLPC lipid monolayer at the air/salt solution (100 mM) and the air/DI water interface with the surface pressures of 10 mN/m.

Table S5. The $\chi^{(2)}_{ppp}(2965cm^{-1})/\chi^{(2)}_{ssp}(2875cm^{-1})$ and the orientation of terminal methyl group of DLPC lipid monolayer at the air/salt solution (100 mM) and the air/DI water interface with the surface pressures of 10 mN/m.

Salts	Water	K_2SO_4	KCl	KBr	KNO_3	KI	$KClO_4$	KSCN
$\frac{\chi^{(2)}_{ppp}(2965cm^{-1})}{\chi^{(2)}_{ssp}(2875cm^{-1})}$	1.38	1.28	1.25	1.27	1.37	1.36	1.33	1.22
θ	21.4	20.7	20.4	20.6	21.4	21.3	21.0	20.2

References

1. Shen, Y. R. The Principles of Nonlinear Optics. Wiley, New York, **1984**.
2. Castellana, E. T.; Cremer, P. S. Solid Supported Lipid Bilayers: From Biophysical Studies to Sensor Design. *Surf. Sci. Rep.* **2006**, *61*, 429-444.
3. Lambert, A. G.; Davies, P. B.; Neivandt, D. J. Implementing the Theory of Sum Frequency Generation Vibrational Spectroscopy: A Tutorial Review. *Appl. Spectrosc. Rev.* **2005**, *40*, 103-145.
4. Gopalakrishnan, S.; Liu, D. F.; Allen, H. C.; Kuo, M.; Shultz, M. J. Vibrational Spectroscopic Studies of Aqueous Interfaces: Salts, Acids, Bases, and Nanodrops. *Chem. Rev.* **2006**, *106*, 1155-1175.
5. Wang, J.; Chen, C.; Buck, S. M.; Chen, Z. Molecular Chemical Structure on Poly(methyl methacrylate) (PMMA) Surface Studied by Sum Frequency Generation (SFG) Vibrational Spectroscopy. *J.Phys.Chem. B* **2001**, *105*, 12118-12125.
6. Wang , H. F.; Gan, W.; Lu, R.; Rao, Y.; Wu, B. H. Quantitative Sectral and Orientational Analysis in Surface Sum Frequency Generation Vibrational Spectroscopy (SFG-VS). *Int. Rev. Phys. Chem.* **2005**, *24*, 191-256.
7. Velarde, L.; Wang, H. F. Unique determination of the –CN Group Tilt Angle in Langmuir

Monolayers Using Sum-Frequency Polarization Null Angle and Phase. *Chem. Phys. Lett.* **2013**, 585, 42-48.

8. Gan, W.; Wu, B. H.; Chen, H.; Guo, Y.; Wang, H. F. Accuracy and Sensitivity of Determining Molecular Orientation at Interfaces Using Sum Frequency Generation Vibrational Spectroscopy. *Chem. Phys. Lett.* **2005**, 406, 467-473.

9. Shultz, M. J.; Bisson, P.; Groenzin, H.; Li, I. Multiplexed Polarization Spectroscopy: Measuring Surface Hyperpolarizability Orientation. *J. Chem. Phys.* **2010**, 133, 054702.

10. Sung, W.; Kim, D.; Shen, Y. Sum-Frequency Vibrational Spectroscopic Studies of Langmuir Monolayers. *Curr. Appl. Phys.* **2013**, 13, 619-632.

11. Rao, Y.; Tao, Y.S.; Wang, H.F. Quantitative Analysis of Orientational Order in the Molecular Monolayer by Surface Second Harmonic Generation. *J.Chem.Phys.* **2003**, 119, 5226-5236.

12. Lu, R.; Gan, W.; Wang H.F. LETTER TO CSB. *Chin. Sci. Bull.* **2004**, 49, 899.

13. Ma, G.; Allen, H. C. DPPC Langmuir Monolayer at the Air-Water Interface: Probing the Tail and Head Groups by Vibrational Sum Frequency Generation Spectroscopy. *Langmuir* **2006**, *22*, 5341-5349.

14. Ma, S.L.; Li, H.C.; Tian, K.Z.; Ye, S.J.; Luo, Y. In Situ and Real Time SFG Measurements Reveal Organization and Transport of Cholesterol Analog 6-Ketocholestanol in Cell Membrane. *J. Phys. Chem. Lett.* **2014***, 5,* 419-424.